Relative and absolute bond dissociation energies of sodium cation–alcohol complexes determined using competitive collision-induced dissociation experiments

Jay C. Amicangelo [a], P.B. Armentrout [b],*

[a] Penn State Erie, School of Science, 4205 College Dr., Erie, PA 16563, United States
[b] Department of Chemistry, University of Utah, 315 S. 1400 E. Rm 2020, Salt Lake City, UT 84112, United States

ARTICLE INFO

ABSTRACT

Absolute $(R_1OH)Na^+–(R_2OH)$ and relative $Na^+–(ROH)$ bond dissociation energies are determined experimentally by competitive collision-induced dissociation of $(R_1OH)Na^+(R_2OH)$ complexes with xenon in a guided ion beam mass spectrometer. The alcohols examined include ethanol, 1-propanol, 2-propanol, n-butanol, iso-butanol, sec-butanol, and $tert$-butanol, which cover a range in Na^+ affinities of only 11 kJ/mol. Dissociation cross sections for formation of $Na^+(R_1OH) + R_2OH$ and $Na^+(R_2OH) + R_1OH$ are simultaneously analyzed with a model that uses statistical theory to predict the energy dependent branching ratio. The cross section thresholds thus determined are interpreted to yield the $0\,K$ $(R_1OH)Na^+–(R_2OH)$ bond dissociation energies and the relative $0\,K$ $Na^+–(ROH)$ binding affinities. The relative binding affinities are converted to absolute $0\,K$ $Na^+–(ROH)$ binding energies by using the absolute bond energy for $Na^+–C_2H_5OH$ determined previously in our laboratory as an anchor value. Comparisons are made to previous experimental and theoretical $Na^+–(ROH)$ thermochemistry from several sources. The absolute $(R_1OH)Na^+–(R_2OH)$ bond dissociation energies were also calculated using quantum chemical theory at the MP2(full)/6-311+G(2d,2p)//MP2(full)/6-31G(d) level (corrected for zero-point energies and basis set superposition errors) and are generally in good agreement with the experimentally determined values.

© 2010 Elsevier B.V. All rights reserved.

1. Introduction

In the last decade, there have been several reviews and comprehensive studies regarding the gas-phase thermochemistry (both experimental and theoretical) of sodium cations with small organic molecules [1–7]. The interest in this topic is a result of the importance of the sodium cation in biological systems [8], as well as the increased use of gas-phase sodium cations in biological applications of mass spectrometry [9]. Knowledge of accurate, absolute thermochemistry for sodium cation complexes is necessary for a complete understanding of the participation and binding characteristics of sodium ions in various biological systems. Sodium cation ligand complexes are also good systems to explore fundamental means of determining accurate thermodynamic information.

We have previously reported accurate $Na^+–L$ bond dissociation energies (BDEs) for $L = H_2O$, C_6H_6, CH_3OH, CH_3OCH_3, NH_3, and C_2H_5OH, determined using competitive collision-induced dissociation (CCID) experiments of doubly ligated sodium cation complexes $(L_1Na^+L_2)$ [10]. This CCID study was undertaken because there

was some disagreement in the literature, including previous work from our laboratory, over the absolute and relative bond dissociation energies for the sodium cation to several of these ligands [2]. Most notable were the discrepancies for the relative BDEs of the sodium cation with benzene and water measured using several different experimental techniques, such as high-pressure mass spectrometry [11–13], FT-ICR equilibrium experiments [4], and collision-induced dissociation (CID) studies [2,14,15]. As a result of the CCID experiments, we were able to refine our previous absolute $Na^+–L$ binding enthalpies for the ligands mentioned above and resolve the discrepancies with the literature values. With the success of the CCID method in refining these absolute $Na^+–L$ BDEs, we then proceeded to closely examine the available published experimental and theoretical absolute BDEs for the sodium cation with the short chain alcohols [2,4,5,7,16] and realized that there was again some disagreement among the various methods and theoretical treatments.

The present experiments were undertaken in an effort to determine more accurate relative and absolute $Na^+–(ROH)$ BDEs for 1-propanol (1-PrOH), 2-propanol (2-PrOH), n-butanol (n-BuOH), iso-butanol (i-BuOH), sec-butanol (s-BuOH), and $tert$-butanol (t-BuOH) by examining CID experiments on doubly ligated alcohol complexes of the sodium cation, $(R_1OH)Na^+(R_2OH)$. The competi-

tive dissociation channels have been simultaneously analyzed to yield absolute $(R_1OH)Na^+$–(R_2OH) and relative Na^+–(ROH) bond dissociation energies at 0 K. From the relative Na^+–(ROH) binding affinities and the use of an absolute anchor, $D_0[Na^+$–$(EtOH)]$, determined from previous competitive CID experiments in our laboratory [10], the absolute Na^+–(ROH) binding energies for these ligands are obtained. The absolute Na^+–(ROH) binding energies determined in this work are compared with available experimental and theoretical literature values and are found to be in good agreement. The absolute $(R_1OH)Na^+$–(R_2OH) bond energies are also calculated using ab initio methods at the MP2(full)/6-311+G(2d,2p)//MP2(full)/6-31G(d) level and are compared with the experimental values.

2. Experimental and computational methods

2.1. General

The guided ion beam instrument on which these experiments were performed has been described in detail previously [17–19]. Briefly, ions are created in a dc-discharge/flow tube ion source, as described below. After extraction from the source, the ions are accelerated and passed through a magnetic sector for mass analysis. The mass-selected ions are then decelerated to the desired kinetic energy and focused into an octopole ion beam guide. This device uses radio-frequency (rf) electric fields to trap the ions in the radial direction and ensure complete collection of reactant and product ions [20,21]. The current arrangement consists of two consecutive octopole ion guides, having lengths 22.9 and 63.5 cm, with a distance between them of 1.0 mm. The rf voltage is the same for the two octopoles but the dc voltage on the second octopole is slightly more negative by 0.3 V for the current experiments. The first octopole passes through a gas collision cell of effective length 8.26 cm that contains the neutral collision partner, Xe here, at a fairly low pressure (0.05–0.2 mTorr). The unreacted parent and product ions drift to the end of the second octopole from which they are extracted, passed through a quadrupole mass filter for mass analysis, and detected with a secondary electron scintillation ion detector using standard pulse counting techniques. Raw ion intensities are converted to cross sections as described previously [17]. Absolute cross section magnitudes are estimated to be accurate to ±20%, while relative cross sections are accurate to ±5%.

Laboratory (lab) energies are converted to center-of-mass (CM) energies using the conversion $E_{CM} = E_{lab} M/(M + m)$, where M and m are the reactant neutral and ion masses, respectively. All energies cited below are in the CM frame unless otherwise noted. The absolute energy scale and corresponding full width at half-maximum (fwhm) of the ion beam kinetic energy distribution are determined using the octopole as a retarding energy analyzer as described previously [17]. Because the reaction zone and the energy analysis region are physically the same, ambiguities in the energy analysis resulting from contact potentials, space charge effects, and focussing aberrations are minimized [17]. The energy distributions are nearly Gaussian and have typical fwhms of 0.2–0.4 eV (lab).

It has been shown previously [22–24] that the shape of collision-induced dissociation (CID) cross sections of ionic complexes is often affected by multiple collisions with the neutral reactant gas, even when the neutral gas pressure is fairly low. Because the presence and magnitude of these pressure effects is difficult to predict, we measured the pressure dependence of all cross sections examined here. Three xenon pressures were used, approximately 0.20, 0.10, and 0.05 mTorr, for all of the $(R_1OH)Na^+(R_2OH)$ systems. All cross sections shown below and all threshold analyses reported here are for data that have been extrapolated to zero reactant pressure, as

described previously [23], and therefore represent rigorous single collision conditions.

2.2. Ion source

The sodium cation complexes are formed in a 1 m long flow tube [18,23] operating at a pressure of 0.6–0.9 Torr with helium flow rates of 6500–8500 sccm. Sodium ions are generated in a continuous dc discharge by argon ion sputtering of a tantalum cathode with a cavity containing sodium metal. Typical operating conditions of the discharge source are 1.8–2.5 kV and 12–22 mA in a flow of roughly 10% argon in helium. Vapors of the alcohol ligands are introduced into the flow approximately 50 cm downstream from the dc discharge. The $(R_1OH)Na^+(R_2OH)$ complexes are formed by associative reactions of the sodium cations with the neutral ligands and are stabilized by collisions with the surrounding bath gas. The flow conditions used in this ion source provide greater than 10^4 collisions with the He buffer gas, such that the ions are believed to be thermalized to 300 K, both vibrationally and rotationally. In our analysis of the data, we assume that the ions are in their ground electronic states and that their internal energy is well characterized by a Maxwell–Boltzmann distribution of ro-vibrational states at 300 K. Previous work from this laboratory has shown that these assumptions are generally valid [22–28].

2.3. Thermochemical analysis

As described in detail previously [29], the threshold regions of the competitive collision-induced dissociation cross sections are modeled using Eq. (1),

$$\sigma_j(E) = \left(\frac{n\sigma_{0,j}}{E}\right) \sum_i g_i \int_{E_{0,j}-E_i}^{E} \left[\frac{k_j(E^*)}{k_{tot}(E^*)}\right] \left[1 - e^{-k_{tot}(E^*)\tau}\right]$$
$$\times (E - \varepsilon)^{n-1} \, d(\varepsilon) \tag{1}$$

where n is an adjustable parameter that describes the energy deposition efficiency during collision [19], $\sigma_{0,j}$ is an energy-independent scaling factor for channel j, E is the relative translational energy of the reactant ion and neutral, $E_{0,j}$ is the CID threshold at 0 K for channel j, τ is the experimental time for dissociation ($\sim 5 \times 10^{-4}$ s in the dual octopole), ε is the energy transferred from translation into internal energy of the complex during the collision between the reactants, and E^* is internal energy of the energized molecule (EM) after the collision, i.e., $E^* = E_i + \varepsilon$. The term $k_j(E^*)$ is the unimolecular rate constant for dissociation to channel j. This rate constant and $k_{tot}(E^*)$ are defined using Rice–Ramsperger–Kassel–Marcus (RRKM) theory [30–32] as,

$$k_{tot}(E^*) = \sum_j k_j(E^*) = \sum_j \frac{d_j N_j^\dagger(E^* - E_{0,m})}{h\rho(E^*)} \tag{2}$$

where d_j is the reaction degeneracy, $N_j^\dagger(E^* - E_{0,j})$ is the sum of ro-vibrational states of the transition state (TS) for channel j at an energy $E^* - E_{0,j}$, and $\rho(E^*)$ is the density of states of the EM at the available energy, E^*. The summation in Eq. (1) is over the ro-vibrational states of the reactant ion, i, where E_i and g_i are the energy and the population ($\sum g_i = 1$) of each state, respectively. The populations of ro-vibrational excited levels are not negligible at 300 K as a result of the many low-frequency modes present in these $(R_1OH)Na^+(R_2OH)$ complexes. The relative reactivities of all ro-vibrational states, as reflected by the parameters $\sigma_{0,j}$ and n, are assumed to be equivalent. Vibrational frequencies (Table 1S) and rotational constants (Table 2S) for the $(R_1OH)Na^+(R_2OH)$ complexes are taken from quantum chemical calculations and scaled to bring the calculated frequencies into general agreement with

the experimentally determined frequencies as found elsewhere [33,34]. The Beyer–Swinehart algorithm [35–37] is used to evaluate the ro-vibrational density of states of the reactant ions and the relative populations, g_i, are calculated for a Maxwell–Boltzmann distribution at 300 K. The scaled vibrational frequencies for the reactants and all products were simultaneously increased and decreased by 10%, in order to estimate errors in the calculated frequencies. The uncertainty that this introduces into the analysis is included in the final uncertainties listed for the CID thresholds, $E_{0,j}$, and the other fitting parameters.

As mentioned above and described in detail elsewhere [25,26,38,39], statistical theories are used to determine the unimolecular rate constants for dissociation. This requires ro-vibrational frequencies for the energized molecules and the transition states (TS) leading to dissociation. Because the metal–alcohol interactions in the $(R_1OH)Na^+(R_2OH)$ complexes are largely electrostatic, the most appropriate model for the TS is a loose association of the ion and neutral alcohol fragments. This TS is located at the centrifugal barrier for the interaction of $(R_1OH)Na^+$ with R_2OH and $(R_2OH)Na^+$ with R_1OH. Therefore, the TS vibrations used here are the frequencies corresponding to the dissociation products. The previously calculated vibrational frequencies for $Na^+(ROH)$ and ROH were used here [16]. The transitional modes, those that become rotations of the completely dissociated products, are treated as rotors, a treatment that corresponds to a phase space limit (PSL), described in detail elsewhere [38,39]. The two-dimensional (2D) external rotations of the TS are treated adiabatically, but with centrifugal effects included [40]. The rotational constants of the energized molecule and the transition state for each $(R_1OH)Na^+(R_2OH)$ complex are listed in Table 2S.

The basic form of Eq. (1) is expected to be appropriate for translationally driven reactions [41] and has been found to reproduce reaction cross sections well for a number of previous studies of both atom-diatom and polyatomic reactions [42], including CID processes [2,14,15,24–28,38,43–48]. The model of Eq. (1) is convoluted with the kinetic energy distribution of the reactants before comparison to the data. The parameters $\sigma_{0,j}$, n, and $E_{0,j}$ are optimized by performing a nonlinear least-squares analysis of the data. An estimate of the error associated with the measurement of $E_{0,j}$ is determined from the range of threshold values obtained for different data sets, for variation of the parameter n, for variations associated with the ±10% uncertainties in the vibrational frequencies, for the effects of increasing and decreasing the time available for the ions to dissociate (5×10^{-4} s) by factors of 2, and for the error in the absolute energy scale, ±0.05 eV (lab).

Because all sources of internal energy are included in the data analysis of Eq. (1), the thresholds obtained correspond to the minimum energy necessary for dissociation, in other words, the 0 K value. This assumption has been tested for several systems [24–28,46]. It has been shown that treating all of the energy of the ion (vibrational, rotational, and translational) as capable of coupling with the reaction coordinate leads to reasonable thermochemistry. The 0 K threshold energies for the CID reactions of $(R_1OH)Na^+(R_2OH)$ with Xe, $E_{0,j}$, are converted to 0 K bond dissociation energies (BDEs), $D_{0,j}$, by assuming that $E_{0,j}$ represents the energy difference between reactants and products at 0 K [25]. This assumption requires that there are no activation barriers in excess of the bond endothermicities, which is generally true for ion-molecule reactions [42] and should be true for the simple heterolytic bond fission reactions examined here [49].

2.4. Computational details

Quantum chemical calculations were performed using Gaussian 98 [50] for the $(R_1OH)Na^+(R_2OH)$ complex ions in order to obtain geometrical structures, vibrational frequencies, rotational

constants, and the energetics of dissociation of the ions. Geometry optimizations were performed first at the RHF/6-31G(d) level, followed by optimization at the MP2(full)/6-31G(d) level. It has been demonstrated that the MP2(full)/6-31G(d) level provides a reasonably good geometrical description of sodium cation complexes with various ligands [1,2,4]. Vibrational frequencies and rotational constants of the $(R_1OH)Na^+(R_2OH)$ complexes were also determined at the MP2(full)/6-31G(d) level. The lowest frequency for the $(R_1OH)Na^+(R_2OH)$ complexes was calculated to be a very low positive value ($8–18\ cm^{-1}$) and corresponds to the synchronous torsional motion of the two ligands about the $(R_1OH)–Na^+–(R_2OH)$ bond axis. For all $(R_1OH)Na^+(R_2OH)$ complexes, our data analysis treated this motion as a one dimensional internal rotor, $I_{torsion} = I_1 I_2 / (I_1 + I_2)$, as described by Gilbert and Smith [30]. When used to model data or calculate thermal energy corrections, the MP2(full)/6-31G(d) calculated vibrational frequencies were scaled by a factor of 0.9646 [51].
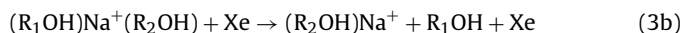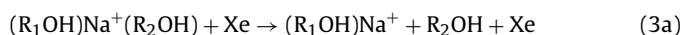
In order to determine the $(R_1OH)Na^+(R_2OH)$ bond energetics, single-point energy calculations were performed at the MP2(full)/6-311+G(2d,2p) level using the MP2(full)/6-31G(d) optimized geometries of the $(R_1OH)Na^+(R_2OH)$ complexes. Using these energies and the energies of the sodium ion and the two neutral ligands, calculated at the same level, the bond energy sum for complete dissociation, i.e., $Na^+–(R_1OH)(R_2OH)$, was calculated. Basis set superposition errors (BSSE) in the calculated $Na^+–(R_1OH)(R_2OH)$ binding energies were estimated using the full counterpoise correction method [52,53]. The BSSE corrections ranged from 13.0 kJ/mol for $(EtOH)Na^+(2\text{-}PrOH)$ to 18.3 kJ/mol for $(1\text{-}PrOH)Na^+(i\text{-}BuOH)$. The calculated $Na^+–(R_1OH)(R_2OH)$ BDEs were also corrected for zero-point energies (ZPEs) using the scaled vibrational frequencies calculated at the MP2(full)/6-31G(d) level. The BSSE and ZPE corrected $Na^+–(R_1OH)(R_2OH)$ BDEs were then combined with the previous theoretical $Na^+–(ROH)$ BDEs calculated at the same level of theory and corrected for ZPE and BSSE [2] to afford the desired $(R_1OH)Na^+–(R_2OH)$ and $(R_2OH)Na^+–(R_1OH)$ BDEs.

3. Results

3.1. Collision-induced dissociation of $(R_1OH)Na^+(R_2OH)$

Collision-induced dissociation cross sections were obtained for 12 doubly ligated complexes of the sodium cation with alcohols, $(R_1OH)Na^+(R_2OH)$, where R_1OH, R_2OH=EtOH, 1-PrOH, 2-PrOH, n-BuOH, i-BuOH, s-BuOH, t-BuOH, reacting with xenon. No systems where $R_1OH=R_2OH$ were studied in the present work. Representative CID data are shown in Fig. 1 for the $(2\text{-}PrOH)Na^+(i\text{-}BuOH)$, $(1\text{-}PrOH)Na^+(n\text{-}BuOH)$, $(EtOH)Na^+(2\text{-}PrOH)$, and $(EtOH)Na^+(t\text{-}BuOH)$ complexes. The CID data of the eight remaining $(R_1OH)Na^+(R_2OH)$ systems examined can be obtained from Figure 1S of the Supplementary Data.

The dominant processes observed for all systems are the losses of the intact ligands, reaction (3), over the energy ranges examined, 0–4 eV.

$$(R_1OH)Na^+(R_2OH) + Xe \rightarrow (R_1OH)Na^+ + R_2OH + Xe \quad (3a)$$

$$(R_1OH)Na^+(R_2OH) + Xe \rightarrow (R_2OH)Na^+ + R_1OH + Xe \quad (3b)$$

The CID cross sections displayed in Fig. 1 are typical results observed in our laboratory for competitive dissociation of doubly ligated metal ion complexes [10,29]. In these systems, the cross sections for the formation of the lowest energy process rise rapidly from baseline with increasing energy. The cross sections then begin to level off and decline at higher energies. The higher energy $Na^+(ROH)$ products have cross sections that rise more slowly than the lower energy channels, but their increases correspond with the leveling off and decline of the first product channel cross sec-
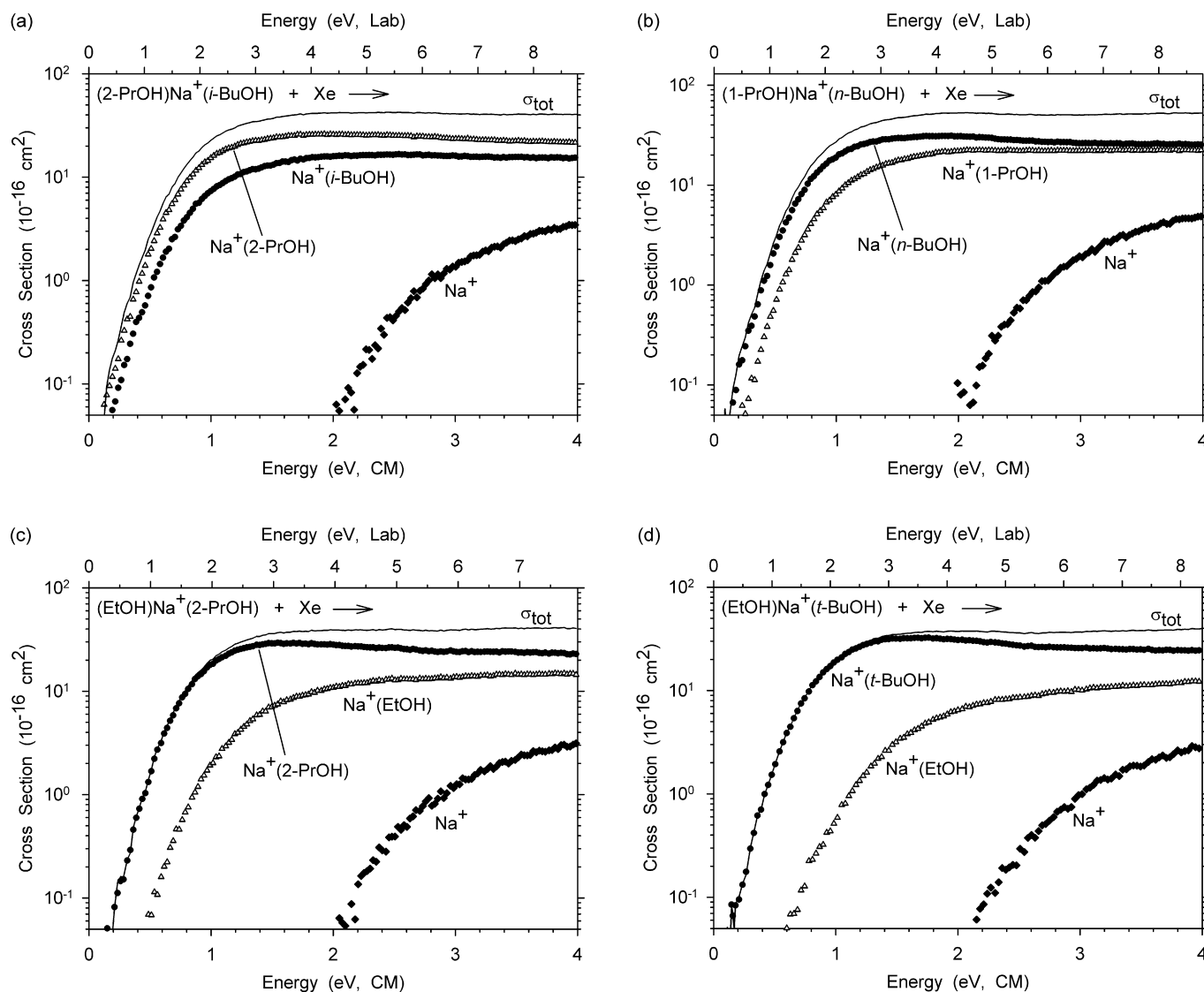
Fig. 1. Cross sections for collision-induced dissociation of (a) (2-PrOH)Na$^+$(i-BuOH), (b) (1-PrOH)Na$^+$(n-BuOH), (c) (EtOH)Na$^+$(2-PrOH), and (d) (EtOH)Na$^+$(t-BuOH) with xenon as a function of kinetic energy in the center-of-mass frame (lower axis) and laboratory frame (upper axis). Solid lines show the total cross section for each system and the symbols represent data extrapolated to zero pressure.

tions. This behavior indicates that the two dissociation channels are indeed in competition with one another. Another sign of this competition is the smooth increases in the total cross sections as energy is varied. At the highest energies examined, the sequential loss of both ligands can occur, forming Na$^+$.

3.2. Competitive threshold analysis

In a previous competitive CID study for (R$_1$OH)Li$^+$(R$_2$OH) complexes using guided ion beam mass spectrometry [29], we showed that the best measure of the dissociation thresholds, $E_{0,j}$, for metal–ligand complex ions in which competition occurs comes from the simultaneous analysis of the cross sections for these dissociation products, reactions (3) in the current (R$_1$OH)Na$^+$(R$_2$OH) systems. These competitive CID processes were analyzed using Eq. (1) with explicit integration over the rotational energy distribution [39,54] and the two cross sections were modeled using a single scaling factor, $\sigma_{0,j}$, for the two channels such that the energy dependent ratio of the cross section magnitudes is determined solely by the statistical rate constant ratio, $k_j(E^*)/k_{tot}(E^*)$. In our earlier study of the competitive CID of L$_1$Na$^+$L$_2$ complexes,

it was shown that the former constraint was necessary in order to obtain a consistent set of relative and absolute Na$^+$–L bond dissociation energies [10]. The results of the competitive threshold analyses for the (R$_1$OH)Na$^+$(R$_2$OH) complexes are presented in Table 1 and representative fits using Eq. (1) are shown in Fig. 2 for (2-PrOH)Na$^+$(i-BuOH), (1-PrOH)Na$^+$(n-BuOH), (EtOH)Na$^+$(2-PrOH), and (EtOH)Na$^+$(t-BuOH). Representative fits using Eq. (1) for all other (R$_1$OH)Na$^+$(R$_2$OH) complexes are given in Fig. 2S of the Supplementary Data. As can be seen from Figs. 2 and 2S, good reproduction of the data is obtained over energy ranges up to 1.2–1.6 eV and over cross section magnitudes of at least a factor of 100 for all complexes.

3.3. Relative and absolute Na$^+$–(ROH) bond dissociation energies

Measurements of the threshold energies for the dissociation processes in reaction (3) provide absolute metal–ligand bond energies for the second ligand, as well as relative bond energies for the doubly ligated metal ion complexes, $\Delta E_0 = D_0(L_2M^+–L_1) – D_0(L_1M^+–L_2)$ [10,29]. Because the sum of the two bond energies is independent of the order in which

Table 1
Competitive fitting parameters of Eq. (1), threshold dissociation energies at 0 K, relative threshold energies, and entropies of activation at 1000 K of $(R_1OH)Na^+(R_2OH)^a$.

Complex	Ionic product	σ_0	n	E_0 (eV)	ΔE_0 (eV)[b]	$\Delta S^\dagger$ (J/K mol)
$(EtOH)Na^+(1\text{-}PrOH)$	$Na^+(1\text{-}PrOH)$ $Na^+(EtOH)$	73 (3)	1.0 (0.2)	0.97 (0.05)1.00 (0.05)	0.035_7 (0.003)	20 (4) 25 (4)
$(EtOH)Na^+(2\text{-}PrOH)$	$Na^+(2\text{-}PrOH)$ $Na^+(EtOH)$	73 (2)	1.1 (0.2)	0.94 (0.05)1.01 (0.05)	0.067_4 (0.003)	20 (4) 24 (4)
$(EtOH)Na^+(n\text{-}BuOH)$	$Na^+(n\text{-}BuOH)$ $Na^+(EtOH)$	79 (3)	1.0 (0.2)	0.96 (0.05)1.02 (0.05)	0.066_7 (0.003)	19 (4) 27 (4)
$(EtOH)Na^+(i\text{-}BuOH)$	$Na^+(i\text{-}BuOH)$ $Na^+(EtOH)$	83 (4)	1.1 (0.2)	0.94 (0.05)1.01 (0.05)	0.067_1 (0.003)	22 (4) 32 (4)
$(EtOH)Na^+(s\text{-}BuOH)$	$Na^+(s\text{-}BuOH)$ $Na^+(EtOH)$	85 (4)	1.0 (0.2)	0.98 (0.05)1.09 (0.05)	0.111_7 (0.004)	19 (4) 28 (4)
$(EtOH)Na^+(t\text{-}BuOH)$	$Na^+(t\text{-}BuOH)$ $Na^+(EtOH)$	72 (2)	1.2 (0.2)	0.92 (0.04)1.04 (0.04)	0.113_1 (0.003)	20 (4) 26 (4)
$(1\text{-}PrOH)Na^+(n\text{-}BuOH)$	$Na^+(n\text{-}BuOH)Na^+(1\text{-}PrOH)$	84 (8)	1.1 (0.2)	0.93 (0.05)0.96 (0.05)	0.028_7 (0.003)	25 (4) 29 (4)
$(1\text{-}PrOH)Na^+(i\text{-}BuOH)$	$Na^+(i\text{-}BuOH)Na^+(1\text{-}PrOH)$	79 (8)	1.1 (0.2)	0.93 (0.05)0.96 (0.05)	0.029_6 (0.003)	27 (4) 33 (4)
$(2\text{-}PrOH)Na^+(n\text{-}BuOH)$	$Na^+(2\text{-}PrOH)Na^+(n\text{-}BuOH)$	69 (2)	1.1 (0.2)	0.97 (0.05)0.97 (0.05)	0.0028 (0.0007)	27 (4) 33 (4)
$(2\text{-}PrOH)Na^+(i\text{-}BuOH)$	$Na^+(2\text{-}PrOH)Na^+(i\text{-}BuOH)$	73 (3)	1.3 (0.3)	0.92 (0.06)0.92 (0.06)	0.001_4 (0.001)	33 (4) 27 (4)
$(2\text{-}PrOH)Na^+(s\text{-}BuOH)$	$Na^+(s\text{-}BuOH)Na^+(2\text{-}PrOH)$	75 (7)	1.2 (0.3)	0.95 (0.07)0.98 (0.07)	0.036_0 (0.002)	23 (4) 28 (4)
$(2\text{-}PrOH)Na^+(t\text{-}BuOH)$	$Na^+(t\text{-}BuOH)Na^+(2\text{-}PrOH)$	68 (5)	1.2 (0.3)	0.95 (0.09)1.00 (0.09)	0.047_8 (0.004)	20 (4) 23 (4)

[a] Uncertainties in parenthesis.
[b] The digit past the uncertainty is indicated as a subscript.

the ligands are removed, ΔE_0 also equals the relative binding energy of the metal ion to the two individual ligands, $D_0(M^+–L_1)–D_0(M^+–L_2)$. The relative thresholds, ΔE_0, determined here for the $(R_1OH)Na^+(R_2OH)$ complexes are given in Table 1. The relative $M^+–L$ bond energies can then be converted to absolute $M^+–L$ bond energies using a reliable absolute metal ion–ligand bond energy as an anchor value. The advantage of using competitive CID of doubly ligated metal ion complexes to determine the absolute BDEs of singly ligated metal ion complexes is that the relative thresholds measured using this method are more precise than those determined from independent absolute CID measurements [10,29]. Such measurements are particularly useful in resolving discrepancies in the literature or for relative binding energies that are smaller than the uncertainties obtained in the absolute CID measurements, which are typically ±0.05–0.10 eV. For the present work, we have chosen our anchor value as the absolute $Na^+–EtOH$ bond dissociation energy, 110.0 ± 5.5 kJ/mol, previously determined in our laboratory using competitive CID [10]. To determine the best set of relative $Na^+–(ROH)$ binding affinities, we use a least-squares minimization of the deviations (χ^2) of the relative values from the experimental relative thresholds (referenced to EtOH as zero) using

the procedure detailed by DeTuri and Ervin [54]. The set of relative $Na^+–(ROH)$ binding energies resulting from this minimization procedure are listed in Table 2 for the seven alcohols studied in this work. To determine absolute $Na^+–(ROH)$ binding energies, the relative binding energies are combined with the absolute anchor value for $Na^+–EtOH$ and these values are also listed in Table 2.

3.4. Theoretical results

The structures for all the $(R_1OH)Na^+(R_2OH)$ complexes studied experimentally were calculated at the MP2(full)/6-31G(d) level of theory. Details of the final optimized geometries are given in Table 3 for all the $(R_1OH)Na^+(R_2OH)$ complexes and the pictorial representations of the optimized structures of $(EtOH)Na^+(n\text{-}BuOH)$, $(EtOH)Na^+(s\text{-}BuOH)$, $(1\text{-}PrOH)Na^+(i\text{-}BuOH)$, and $(2\text{-}PrOH)Na^+(t\text{-}BuOH)$ are displayed in Fig. 3. The pictorial representations of the optimized structures for the remaining eight $(R_1OH)Na^+(R_2OH)$ complexes are given in Figure 3S of the Supplementary Data.

As can be seen in Table 3, the calculations predict that the $Na^+–O$ distances are essentially equivalent for all alcohols, regardless of the identity, with values between 2.21–2.23 Å. For all of the com-

Table 2
Relative and absolute 0 K $Na^+–(ROH)$ bond dissociation energies (kJ/mol) derived from least-squares minimization of CCID fitting along with literature experimental and theoretical bond dissociation energies[a].

ROH	Experiment				Theory					
	Relative CCID[b]	Absolute CCID[c]	Absolute CID[d]	FT-ICR[e]	MP2[d]	G2[d]	CBS-Q[d]	B3LYP[f]	B3P86[f]	CP-dG2thaw[g]
MeOH	12.7 (1.6)[h]	97.3 (5.5)[h]	91.7 (5.7)	98.4 (5.1) 98.7 (1.6)[i]	100.0	98.5	96.2	105.2	100.8	100.3
EtOH	0.00	110.0 (5.5)[h]	102.0 (3.7)	110.1 (5.1)	108.9	107.6	104.4	114.7	111.1	109.3
1-PrOH	3.55 (0.11)	113.5 (5.5)	108.0 (4.1)	113.5 (5.2)	112.0	112.0	108.7	115.1	111.0	109.8
n-BuOH	6.36 (0.03)	116.3 (5.5)	109.4 (4.7)	114.1 (5.2)	114.5	113.9	109.4	121.8	116.1	
i-BuOH	6.48 (0.03)	116.4 (5.5)	105.2 (5.2)	114.5 (5.2)	112.6	112.0	115.2	119.7	114.5	
2-PrOH	6.63 (0.08)	116.5 (5.5)	113.2 (4.3)	116.5 (5.1)	113.0	109.0	117.0	119.5	115.6	114.6
s-BuOH	10.23 (0.38)	120.2 (5.5)	117.2 (5.1)	123.2 (5.2)	117.1	116.4	118.9	125.0	119.2	
t-BuOH	11.03 (0.23)	121.0 (5.5)	116.5 (4.1)	118.3 (5.2)	116.8	115.7	113.5	123.3	119.0	118.3
MAD CID[j]		6.0 (2.7)		5.8 (2.3)	4.0 (3.4)	4.2 (2.4)	3.3 (3.1)	10.1 (3.4)	5.5 (3.4)	4.2 (3.5)
MAD CCID[k]			6.0 (2.7)	1.4 (1.1)	2.7 (1.1)	3.6 (2.1)	3.8 (2.9)	4.1 (2.0)	1.6 (1.1)	2.4 (1.1)

[a] Uncertainties in experimental values are in parentheses.
[b] Relative BDEs from competitive CID, present work.
[c] Absolute BDEs from competitive CID, present work.
[d] Ref. [16]. MP2 = MP2(full)/6-311+G(2d,2p)//MP2(full)/6-31G(d).
[e] Obtained using experimental ΔG_{298} values from McMahon and Ohanessian [4] and enthalpy and entropy corrections determined at the MP2(full)/6-31G(d) level, Table 5 [16]. For the entropy and 298 to 0 K enthalpic corrections, two of the internal rotors of the neutral alcohols were treated as hindered rotors as described in the text [10,55].
[f] B3LYP = B3LYP/6-311+G(2d,2p)//B3LYP/6-31G(d), B3P86 = B3P86/6-311+G(2d,2p)//B3P86/6-31G(d), Ref. [2].
[g] Values from Ref. [7]. The CP-dG2thaw method is a variation of the standard G2 calculation method that is tailored for calculations involving one or more metal ions. See Ref. [7] and references therein.
[h] Ref. [10].
[i] Obtained using experimental ΔH_{298} reported by Hoyau et al. [1] and an enthalpy correction determined at the MP2(full)/6-31G(d) level [16], but treating the neutral MeOH internal rotor as a hindered rotor.
[j] Mean absolute deviation from direct CID results.
[k] Mean absolute deviation from competitive CID results.
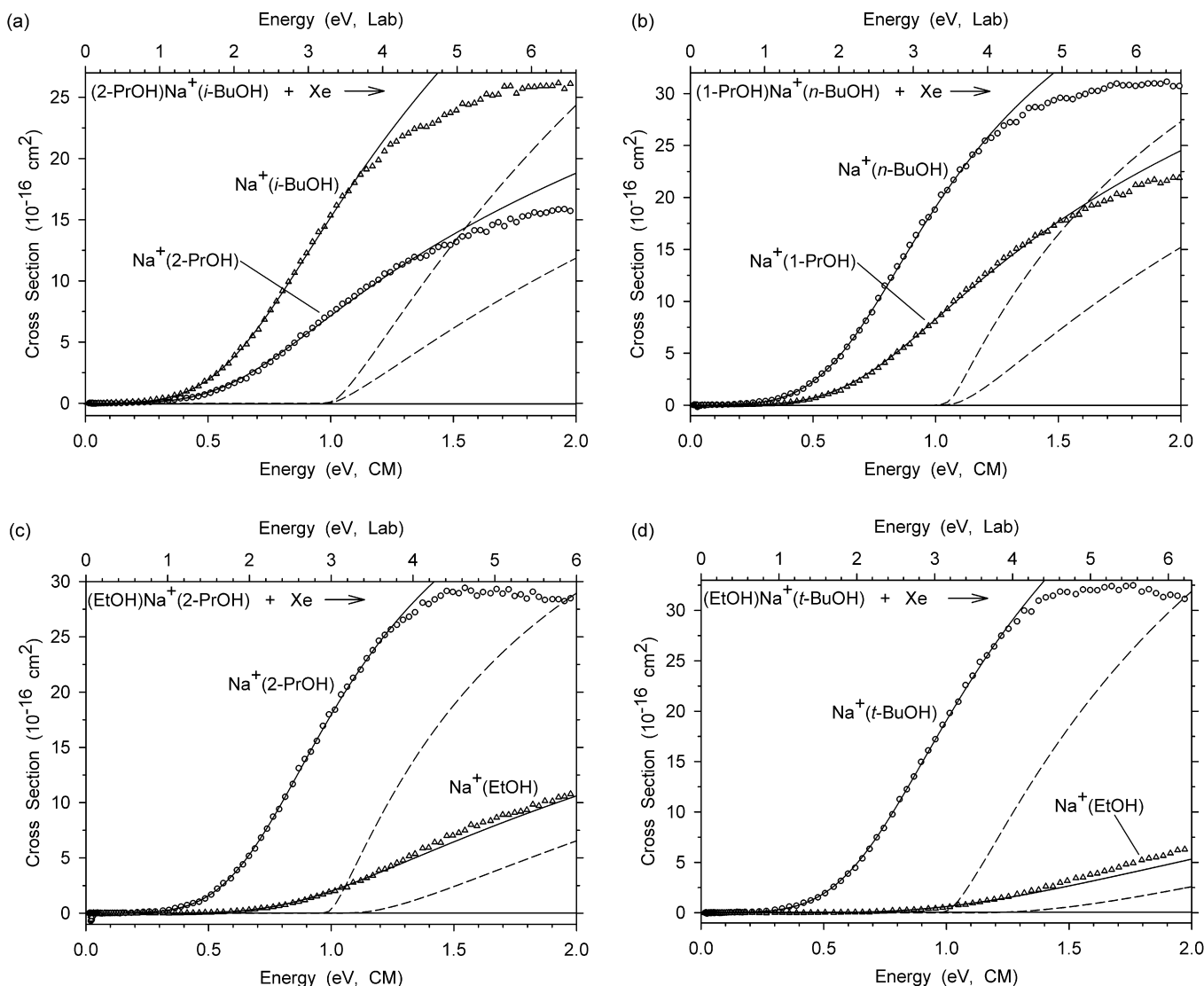
Fig. 2. Zero pressure extrapolated cross sections for the competitive collision-induced dissociation processes of (a) (2-PrOH)Na$^+$(i-BuOH), (b) (1-PrOH)Na$^+$(n-BuOH), (c) (EtOH)Na$^+$(2-PrOH), and (d) (EtOH)Na$^+$(t-BuOH) with xenon in the threshold region as a function of kinetic energy in the center-of-mass frame (lower axis) and laboratory frame (upper axis). Solid lines show the best fits to the data using the model of Eq. (1) convoluted over the neutral and ion kinetic energies and the internal energies of the reactants. Dashed lines show the model cross sections in the absence of experimental energy broadening for reactants with an internal energy of 0 K.

plexes, the O′–Na$^+$–O angles are nearly linear, with values between 175.1° and 178.5°. For the Na$^+$–O–C angles, the values are all predicted to be close to 120°, i.e., along the local dipole moment, with some small systematic differences that appear to be related to the identity of the alcohol. For example, when the alcohol is n-BuOH the Na$^+$–O–C angles are in the range of 117.9–118.2° and when the alcohol is EtOH the Na$^+$–O–C angles are in the range of 121.1–121.2°. The Na$^+$–O distances and Na$^+$–O–C angles determined here for the (R$_1$OH)Na$^+$(R$_2$OH) complexes are also roughly equivalent to those reported previously for the singly ligated Na$^+$–(ROH) complexes with the same alcohols, also calculated at the MP2(full)/6-31G(d) level of theory [16]. This suggests that the binding of the second alcohol does not perturb the geometry of the sodium cation with the first alcohol to a great extent. Also, in all cases, the geometry of the alcohol when complexed to the sodium cation is very close to the geometry of the free alcohol, indicating very little distortion upon complexation. The parameter that varies the most among the (R$_1$OH)Na$^+$(R$_2$OH) complexes is the C′–O′–O–C dihedral angle (which describes the relative orientations of the two alcohol ligands) with values between 67.2° and 82.2°. The optimized structures displayed in Figs. 3 and 3S are the global minima

along the C′–O′–O–C dihedral angle coordinate, as these are the lowest energy structures obtained when geometry optimizations were started with initial dihedral angles set at either 90.0° or 180.0°.

It is interesting that the optimized C′–O′–O–C dihedral angles are all close to 90.0°. A value of 180.0° might be expected to minimize repulsive interactions between the two alcohol ligands. Examination of the geometries of the doubly ligated complexes shows that there are attractive electrostatic interactions between the C$_\beta$H$_x$ groups and the sodium ion, with Na–H distances between 2.46 and 2.85 å. These interactions have been described previously for the complexes containing only a single ligand [16]. Clearly, such interactions must involve electron donation from the alkyl groups to empty orbitals on the sodium cation. If the latter involve the empty 3p orbitals, then donation into distinct 3pπ orbitals would maximize the acceptor ability and lead to geometries having perpendicular dihedral angles, as observed.

Theoretical (R$_1$OH)Na$^+$–(R$_2$OH) bond dissociation energies were calculated using the MP2(full)/6-31G(d) optimized geometries and single-point energy calculations at the MP2(full)/6-311+G(2d,2p) level, with zero-point energy and counterpoint corrections as described above. These values are listed in Table 4 along with the

Table 3
Geometrical parameters of the MP2(full)/6-31G(d) optimized structures of the $(R_1OH)Na^+(R_2OH)$ complexes[a].

Complex	Na$^+$–O distances (Å)[b]	∠O′Na$^+$O (°)	∠Na$^+$OC (°)[b]	∠C′–O′–O–C Dihedral angle (°)
(EtOH)Na$^+$(1-PrOH)	2.22 (E), 2.22 (1P)	176.7	121.1 (E), 119.4 (1P)	80.1
(EtOH)Na$^+$(2-PrOH)	2.22 (E), 2.22 (2P)	176.3	121.2 (E), 121.3 (2P)	81.3
(EtOH)Na$^+$(n-BuOH)	2.23 (E), 2.22 (nB)	177.0	121.2 (E), 118.2 (nB)	77.4
(EtOH)Na$^+$(i-BuOH)	2.23 (E), 2.22 (iB)	175.1	121.1 (E), 119.4 (iB)	69.2
(EtOH)Na$^+$(s-BuOH)	2.23 (E), 2.22 (sB)	177.2	121.1 (E), 120.2 (sB)	82.2
(EtOH)Na$^+$(t-BuOH)	2.23 (E), 2.21 (tB)	176.4	121.2 (E), 121.5 (tB)	79.5
(1-PrOH)Na$^+$(n-BuOH)	2.22 (1P), 2.22 (nB)	178.5	119.3 (1P), 117.9 (nB)	77.6
(1-PrOH)Na$^+$(i-BuOH)	2.22 (1P), 2.22 (iB)	175.9	119.4 (1P), 119.4 (iB)	67.2
(2-PrOH)Na$^+$(n-BuOH)	2.22 (2P), 2.22 (nB)	176.4	121.3 (2P), 118.0 (nB)	78.5
(2-PrOH)Na$^+$(i-BuOH)	2.22 (2P), 2.22 (iB)	175.4	121.2 (2P), 119.3 (iB)	69.3
(2-PrOH)Na$^+$(s-BuOH)	2.22 (2P), 2.22 (sB)	177.1	121.3 (2P), 120.1 (sB)	79.0
(2-PrOH)Na$^+$(t-BuOH)	2.22 (2P), 2.21 (tB)	177.1	121.2 (2P), 121.4 (tB)	80.0

[a] O and O′ are the oxygen atoms in the two alcohols and C and C′ are the carbon atoms bonded to O and O′, respectively.
[b] The designations in parenthesis refer to the alcohol to which the value applies; E = EtOH, 1P = 1-PrOH, 2P = 2-PrOH, nB = n-BuOH, iB = i-BuOH, sB = s-BuOH, tB = t-BuOH.
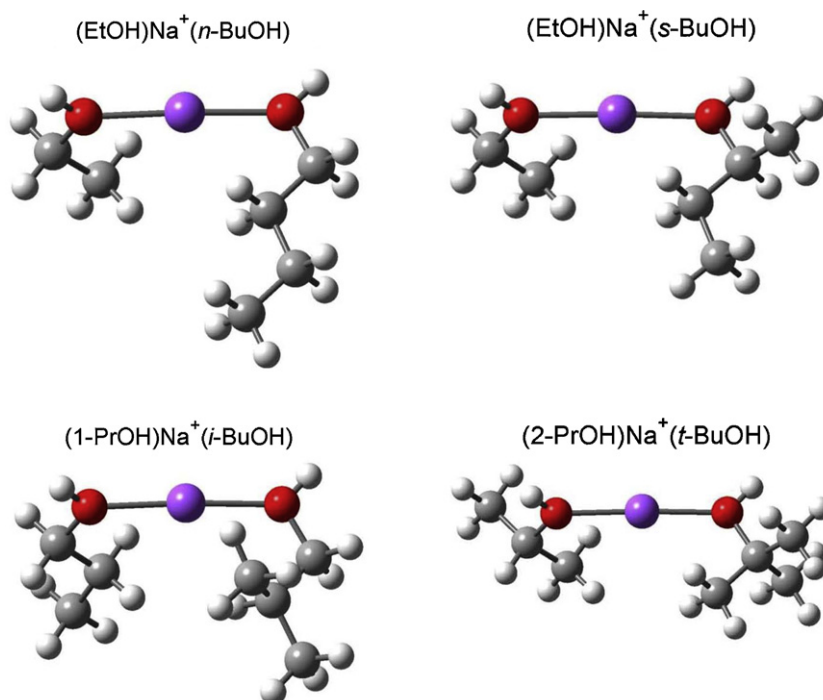
current experimental $(R_1OH)Na^+$–(R_2OH) bond dissociation energy determinations.

4. Discussion

4.1. Relative and absolute Na$^+$–(ROH) bond dissociation energies

The best set of relative Na$^+$–(ROH) BDEs determined from the least-squares minimization of the deviations of all of the competitive threshold analyses (Table 1) are presented in Table 2. From the relative Na$^+$–(ROH) BDEs, absolute Na$^+$–(ROH) BDEs are obtained by using the Na$^+$–EtOH absolute anchor value (110.0 ± 5.5 kJ/mol) and these values are also listed in Table 2. Also listed in Table 2 are experimental BDEs determined from direct CID experiments performed previously in our laboratory [16], experimental BDEs derived from FT-ICR ligand exchange equilibrium experiments [4], and theoretical BDEs calculated at several levels of theory [2,7,16]. Fig. 4 shows each of these correlated with the present absolute CCID values. Although methanol (MeOH) was not part of the current experimental study, the available experimental and theoretical literature values of the absolute Na$^+$–MeOH BDE are included in Table 2 for completeness [1,2,4,7,10,16]. Theoretical Na$^+$–(ROH) BDEs calculated at the B3LYP/6-311+G(2d,2p)//B3LYP/6-31G(d), B3P86/6-311+G(2d,2p)//B3P86/6-31G(d), and G2 levels were previously reported in our group [2,16] but did not include the four butanols. Therefore, the appropriate calculations were performed in the current work in order to have a complete set of calculated Na$^+$–(ROH) BDEs at each level of theory. The literature FT-ICR results [4] are actually free energies of sodium cation binding to the alcohols and were converted to the BDEs listed in Table 2 using enthalpic and entropic correction factors determined primarily from molecular constants obtained at the MP2(full)/6-31G(d) level [16]. In our previous study of the competitive CID of $L_1Na^+L_2$ complexes [10], it was determined that for the calculation of the dissociation entropy and the 298 to 0 K enthalpic conversion of Na$^+$–EtOH, it was necessary to treat the CH$_3$ and OH internal rotations of the neutral EtOH product as hindered rotors rather than as vibrators or free rotors. This same approach was applied to the cal-

Fig. 3. Ground state geometries of (EtOH)Na$^+$(n-BuOH), (EtOH)Na$^+$(s-BuOH), (1-PrOH)Na$^+$(i-BuOH), and (2-PrOH)Na$^+$(t-BuOH) complexes, optimized at the MP2(full)/6-31G(d) level of theory.

Table 4
Experimental and theoretical bond dissociation energies (in kJ/mol) of $(R_1OH)Na^+–(R_2OH)$ at 0 K[a].

R_1OH	R_2OH						
	EtOH	1-PrOH	*n*-BuOH	*i*-BuOH	2-PrOH	*s*-BuOH	*t*-BuOH
None	110.0 (5.5)[b]	113.5 (5.5)[b]	116.3 (5.5)[b]	116.4 (5.5)[b]	116.5 (5.5)[b]	120.2 (5.5)[b]	121.0 (5.5)[b]
	108.9[c]	*112.0[c]*	*114.5[c]*	*112.6[c]*	*113.0[c]*	*117.1[c]*	*116.8[c]*
EtOH		96.5 (4.8)	98.4 (4.8)	97.4 (4.8)	97.4 (4.8)	105.2 (4.8)	100.3 (3.8)
		95.3	*97.4*	*95.0*	*99.3*	*99.5*	*99.5*
1-PrOH	93.6 (4.8)		92.6 (4.8)	92.6 (6.8)			
	92.2		*96.6*	*94.2*			
n-BuOH	92.6 (4.8)	89.7 (4.8)			93.6 (4.8)		
	91.8	*94.1*			*102.7*		
i-BuOH	90.7 (4.8)	89.7 (4.8)			88.8 (5.8)		
	91.3	*93.6*			*94.6*		
2-PrOH	90.7 (4.8)		93.6 (4.8)	88.8 (5.8)		94.6 (6.8)	96.5 (8.7)
	95.2		*104.2*	*94.2*		*98.7*	*98.7*
s-BuOH	94.6 (4.8)				91.7 (6.8)		
	91.3				*94.6*		
t-BuOH	88.8 (3.8)				91.7 (8.7)		
	91.6				*94.9*		

[a] Uncertainties in parentheses. MP2(full)/6-311+G(2d,2p)//MP2(full)/6-31G(d) values including ZPE and BSSE corrections, are in italics. Experimental values taken from Table 1, except as noted.
[b] Absolute CCID values from Table 2.
[c] MP2 values from Ref. [16].

culation of the dissociation entropies and the 298 to 0 K enthalpic conversion factors for all of the Na⁺–(ROH) complexes. Two hindered rotors were used in the treatment of the current set of neutral alcohols, the first being the OH internal rotor for each alcohol and the second being the internal rotor (CH_3, C_2H_5, or C_3H_7) associated with the part of the alkyl chain interacting with the Na⁺ as judged by the optimized Na⁺–(ROH) structures. The hindered rotor parameters for all of the neutral alcohols were taken from the work of Chao et al. [55], which does not include *i*-BuOH. Because the portion of the alkyl chain interacting with the Na⁺ ion in Na⁺–(*i*-BuOH) looks similar to that of Na⁺–(2-PrOH), the hindered rotor parameters for 2-PrOH were used in this case. The enthalpic and entropic correction factors resulting from this procedure for the Na⁺–(ROH) complexes are given in Table 5.

As can be seen from Table 2 and Fig. 4, the agreement between the absolute Na⁺–(ROH) BDEs determined from competitive CID (CCID) with the FT-ICR and all theory values is quite good, with mean absolute deviations (MADs) between 1.4 and 4.1 kJ/mol. Although there is a larger disagreement between the CCID values and those obtained from direct CID measurements (MAD = 6.0 ± 2.7 kJ/mol, eight values), the direct CID values do agree with the current ligand exchange values within the combined uncertainties of the two measurements. Examination of the deviations between the direct CID and CCID values reveals a systematic deviation towards higher values for the CCID BDEs by 3.0–11.2 kJ/mol, which is primarily a result of the shift in the Na⁺–(EtOH) BDE, used as the anchor value in the current study. In an effort to determine the underlying cause of this systematic deviation, particularly for the Na⁺–(EtOH) and Na⁺–(*i*-BuOH) systems which have the largest absolute deviations (8.0 and 11.2 kJ/mol, respectively), we remodeled some of the original data sets for these complexes with two new features currently incorporated
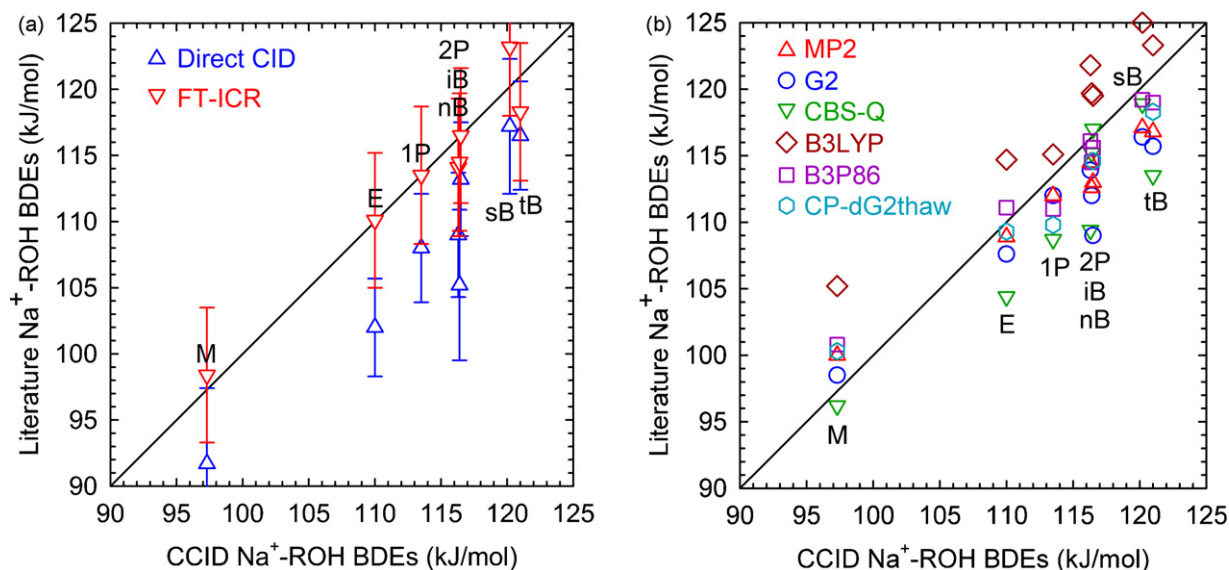
Fig. 4. Absolute 0 K Na⁺–(ROH) bond dissociation energies determined by (a) direct CID (open triangles with error bars, Ref. [16]) and FT-ICR equilibrium studies (open inverted triangles with error bars, Ref. [4]) and (b) theoretical calculations at the MP2(full)/6-311+G(2d,2p)//MP2(full)/6-31G(d) (triangles, Ref. [16]), G2 (circles, Ref. [16] and present work), CBS-Q (inverted triangles, Ref. [16]), B3LYP/6-311+G(2d,2p)//B3LYP/6-31G(d) (diamonds, Ref. [2] and present work), B3P86/6-311+G(2d,2p)//B3P86/6-31G(d) (squares, Ref. [2] and present work), and CP-dG2thaw (hexagons, Ref. [7]) levels of theory versus competitive CID (CCID) bond dissociation energies from Table 2. The diagonal line indicates the values for which literature values are equal to the CCID values. M = MeOH, E = EtOH, 1P = 1-PrOH, 2P = 2-PrOH, nB = *n*-BuOH, iB = *i*-BuOH, sB = *s*-BuOH, tB = *t*-BuOH.

Table 5
Enthalpies and free energies (in kJ/mol) for Na^+–(ROH) at 0 and 298 K[a].

ROH	ΔH_0[b]	$\Delta H_{298} - \Delta H_0$[c]	ΔH_{298}	$T\Delta S_{298}$[c]	ΔG_{298}	ΔG_{298} (FT-ICR)[d]
MeOH	97.3 (5.5)	1.7 (1.4)	99.0 (5.6)	27.7 (4.7)	71.3 (7.3)	72.4 (1.2)
EtOH	110.0 (5.5)	1.5 (1.3)	111.5 (5.6)	32.1 (4.8)	79.4 (7.4)	79.5 (0.9)
1-PrOH	113.5 (5.5)	1.1 (1.1)	114.6 (5.6)	33.0 (5.0)	81.6 (7.5)	81.6 (1.0)
n-BuOH	116.3 (5.5)	1.1 (1.0)	117.4 (5.6)	32.8 (5.0)	84.6 (7.5)	82.4 (1.0)
i-BuOH	116.4 (5.5)	1.2 (1.1)[e]	117.6 (5.6)	33.3 (5.0)[e]	84.3 (7.5)	82.4 (1.0)
2-PrOH	116.5 (5.5)	1.3 (1.2)	117.8 (5.6)	32.4 (5.0)	85.4 (7.4)	85.4 (1.1)
s-BuOH	120.2 (5.5)	0.9 (1.0)	121.1 (5.6)	36.7 (5.0)	84.4 (7.5)	87.4 (1.1)
t-BuOH	121.0 (5.5)	1.2 (1.1)	122.2 (5.6)	30.0 (4.9)	92.2 (7.4)	89.5 (1.3)

[a] Uncertainties in parenthesis.
[b] Present experimental results (absolute CCID values from Table 2).
[c] Calculated using standard formulas and molecular constants determined at the MP2(full)/6-31G(d) level [16]. Uncertainties correspond to increases and decreases in the metal–ligand frequencies by a factor of 2 and ±10% variations in the ligand frequencies. The internal rotors of the neutral alcohols were treated as hindered rotors as described in the text [10,55].
[d] Ref. [4].
[e] Ref. [55] did not have hindered rotor parameters for i-BuOH and the hindered rotor parameters for 2-PrOH were used in this case.

into the CRUNCH program: hindered rotor treatment [10] and the locked-dipole approximation [56]. When the hindered rotor approach is applied to the appropriate two internal rotors of the neutral alcohols as described above, the thresholds increased by 0.5 and 0.2 kJ/mol for the Na^+–(EtOH) and Na^+–(i-BuOH) complexes, respectively. When the hindered rotor approach and locked-dipole approximation (using dipole moments of 1.73 and 1.65 D for EtOH and i-BuOH, respectively [57]) are both applied, the thresholds increased by 1.4 and 1.1 kJ/mol for the Na^+–(EtOH) and Na^+–(i-BuOH) complexes, respectively. This revised analysis moves the direct CID BDEs for Na^+–(EtOH) and Na^+–(i-BuOH) up to values of 103.4 and 106.3 kJ/mol, respectively, which improves the agreement between the direct CID and the CCID values, but clearly not by enough to eliminate the discrepancy.

The direct CID results can also be compared to the literature experimental and theoretical BDEs. As can be seen from Table 2, the agreement is a little worse for the direct CID results than for the CCID results, with MADs between 3.3 and 10.1 kJ/mol. In most cases, the agreement is within the limits of uncertainty. The obvious outlier in the comparison of the direct CID results to the theory is the B3LYP calculated BDEs (MAD = 10.1 ± 3.4 kJ/mol, eight values), which are all systematically higher than the direct CID values. We also note that even though the B3LYP and CCID values agree better (MAD of 4.1 ± 2.0 kJ/mol, eight values), the B3LYP values are still systematically high. Calculations using the B3P86 functional do a much better job at predicting the absolute BDEs, with MADs of 1.6 ± 1.1 and 5.5 ± 3.4 kJ/mol (eight values each) between the CCID and the direct CID results, respectively. The trends observed here are consistent with a comprehensive analysis of various theoretical approaches to calculate accurate sodium cation affinities previously reported by our group [2].

In terms of the order of the absolute Na^+–(ROH) BDEs, the following is observed from the competitive CID measurements: MeOH < EtOH < 1-PrOH < n-BuOH < i-BuOH < 2-PrOH < s-BuOH < t-BuOH. It should be pointed out, however, that the values for n-BuOH, i-BuOH, and 2-PrOH are all very close to one another, with only 0.12 and 0.15 kJ/mol separating the adjacent values. The values derived from the FT-ICR experiments predict nearly the same order of the Na^+–(ROH) BDEs, with the only difference being that the Na^+–t-BuOH BDE is lower than that for Na^+–s-BuOH. As mentioned above, the FT-ICR experiments actually measure the Na^+–(ROH) dissociation free energies. From Table 5, it can be seen that the ΔG_{298} of Na^+–t-BuOH (89.5 ± 1.3 kJ/mol) is larger than that of Na^+–s-BuOH (87.4 ± 1.1 kJ/mol). The reversal in the order of the BDEs results from the entropic terms, which rely primarily on the lowest frequency vibrations and therefore may not be accurately calculated. The order of the Na^+–(ROH) BDEs predicted from the direct CID experiments is also similar to the

CCID order, except that in addition to predicting the reverse order for Na^+–t-BuOH and Na^+–s-BuOH, the Na^+–i-BuOH BDE is below the Na^+–1-PrOH and Na^+–n-BuOH BDEs. Given the closeness of the BDEs from the Na^+–EtOH to the Na^+–t-BuOH complexes (11 kJ/mol) and that typical uncertainties in the direct CID measurements are in the range of 3–6 kJ/mol, it is not surprising that the order of the Na^+–(ROH) BDEs predicted from the direct CID measurements varies somewhat.

Although the present results refine the absolute Na^+–(ROH) BDEs previously determined in our laboratory, it is important to note that these refined values are not significantly different than those determined by direct CID of Na^+(ROH) complexes [16]. In all cases, the differences between the current and previous results are within the combined uncertainties of the two measurements. Because each direct CID study is a completely independent measurement of the absolute Na^+–(ROH) BDEs, determinations of differences between systems with similar absolute BDEs is made much more reliably by equilibrium or competitive CID experiments in which the relative binding is determined directly. In the cases included in this work, for example, the bond energies span a range of only 11 kJ/mol (0.11 eV).

In order to facilitate comparison of our new recommended absolute Na^+–(ROH) binding energies determined using competitive CID to other experiments, we have converted our 0 K values to 298 K enthalpies and free energies. These are given in Table 5 along with the absolute free energies determined using FT-ICR ligand exchange equilibrium experiments [4]. The agreement between the free energies derived from our CCID experiments with those determined from the FT-ICR experiments is excellent, with a MAD of 1.4 ± 1.2 kJ/mol (eight values) and the largest deviation only 3.0 kJ/mol.

4.2. Absolute $(R_1OH)Na^+$–(R_2OH) bond dissociation energies

As mentioned above, the thresholds measured in the present experiments directly yield the absolute second alcohol BDEs to the sodium cation, $(R_1OH)Na^+$–(R_2OH). These values are listed in Table 4 along with theoretical values calculated at the MP2(full)/6-311+G(2d,2p)//MP2(full)/6-31G(d) level of theory including ZPE and BSSE corrections. For all systems studied, the second alcohol ligand is more weakly bound to the sodium cation than the first alcohol ligand, as expected for the electrostatic nature of the bonding in these complexes. The agreement between experiment and theory for these sodium cation complexes is generally within experimental error, with a MAD of 3.5 ± 2.5 kJ/mol (24 values). The comparison between experiment and theory is also represented in Fig. 5, where it can be seen that most of the points are evenly scattered about the diagonal line, which represents equivalent experimental and calculated values. Most values lie within
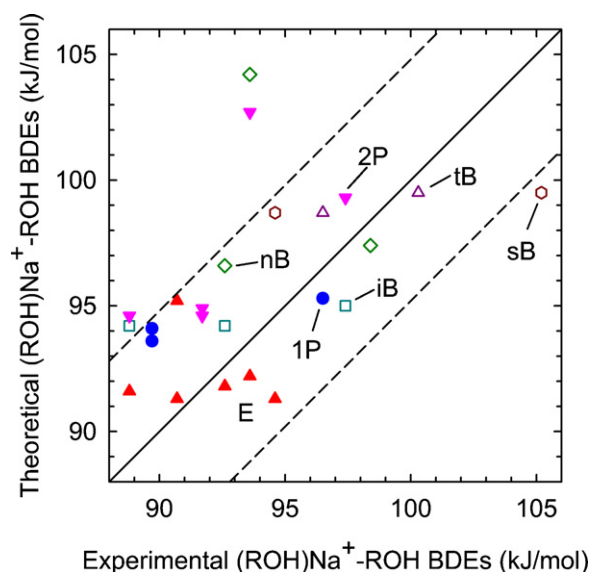
Fig. 5. Experimental versus theoretical absolute 0 K $(R_1OH)Na^+$–(R_2OH) bond dissociation energies, according to the R_2OH ligand: EtOH (E, closed triangles), 1-PrOH (1P, closed circles), n-BuOH (nB, open diamonds), i-BuOH (iB, open squares), 2-PrOH (2P, closed inverted triangles), s-BuOH (sB, open hexagons), and t-BuOH (tB, open triangles). All values are taken from Table 4. The solid diagonal line indicates the values for which measured and calculated values are equal. The dashed diagonal lines indicate an uncertainty of ±4.8 kJ/mol about the solid diagonal line.

the 4.8 kJ/mol uncertainty (indicated by the dashed lines) typical of most values in Table 4. There are two BDEs that clearly show large deviations: $(n$-BuOH$)Na^+$–$(2$-PrOH$)$ and $(2$-PrOH$)Na^+$–$(n$-BuOH$)$. For this complex, the MP2 calculations overestimate the BDEs, although it is unclear why the discrepancies for this particular system is so much larger than the others.

Acknowledgments

Appendix A. Supplementary data

Supplementary data associated with this article can be found, in the online version, at doi:10.1016/j.ijms.2010.06.024.

References

[1] S. Hoyau, K. Norrman, T.B. McMahon, G. Ohanessian, J. Am. Chem. Soc. 121 (1999) 8864.
[2] P.B. Armentrout, M.T. Rodgers, J. Phys. Chem. A 104 (2000) 2238.
[3] M.T. Rodgers, P.B. Armentrout, Mass Spectrom. Rev. 19 (2000) 215.
[4] T.B. McMahon, G. Ohanessian, Chem. Eur. J. 6 (2000) 2931.
[5] F.M. Siu, N.L. Ma, C.W. Tsang, J. Chem. Phys. 114 (2001) 7045.
[6] M.M. Kish, G. Ohanessian, C. Wesdemiotis, Int. J. Mass Spectrom. 227 (2003) 509.
[7] J. Bloomfield, E. Davies, P. Gatt, S. Petrie, J. Phys. Chem. A 110 (2006) 1134.
[8] S.J. Lippard, J.M. Berg, Principles of Bioinorganic Chemistry, University Science Books, Mill Valley, CA, 1994.
[9] For example, see P.C. Liao, J. Allison, J. Mass Spectrom. 30 (1995) 408.
[10] J.C. Amicangelo, P.B. Armentrout, Int. J. Mass Spectrom. 212 (2001) 301.
[11] J.J. Gilligan, L.R. McCunn, B.D. Leskiw, Z. Herman, A.W. Castleman Jr., Int. J. Mass Spectrom. 204 (2001) 247.
[12] B.C. Guo, J.W. Purnell, A.W. Castleman Jr., Chem. Phys. Lett. 168 (1990) 155.
[13] I. Dzidic, P. Kebarle, J. Phys. Chem. 74 (1970) 1466.
[14] J.C. Amicangelo, P.B. Armentrout, J. Phys. Chem. A 104 (2000) 11420.
[15] N.F. Dalleska, B.L. Tjelta, P.B. Armentrout, J. Phys. Chem. 98 (1994) 4191.
[16] M.T. Rodgers, P.B. Armentrout, J. Phys. Chem. A 103 (1999) 4955.
[17] K.M. Ervin, P.B. Armentrout, J. Chem. Phys. 83 (1985) 166.
[18] R.H. Schultz, P.B. Armentrout, Int. J. Mass Spectrom. Ion Processes 107 (1991) 29.
[19] F. Muntean, P.B. Armentrout, J. Chem. Phys. 115 (2001) 1213.
[20] E. Teloy, D. Gerlich, Chem. Phys. 4 (1974) 417.
[21] D. Gerlich, in: C.Y. Ng, M. Baer (Eds.), State-Selected and State-to-State Ion-Molecule Reaction Dynamics, Part 1: Experiment, vol. LXXXII, John Wiley & Sons Inc., New York, 1992, pp. 1–176.
[22] S.K. Loh, L. Lian, D.A. Hales, P.B. Armentrout, J. Chem. Phys. 89 (1988) 3378.
[23] R.H. Schultz, K.C. Crellin, P.B. Armentrout, J. Am. Chem. Soc. 113 (1991) 8590.
[24] N.F. Dalleska, K. Honma, L.S. Sunderlin, P.B. Armentrout, J. Am. Chem. Soc. 116 (1994) 3519.
[25] N.F. Dalleska, K. Honma, P.B. Armentrout, J. Am. Chem. Soc. 115 (1993) 12125.
[26] F.A. Khan, D.E. Clemmer, R.H. Schultz, P.B. Armentrout, J. Phys. Chem. 97 (1993) 7978.
[27] R.H. Schultz, P.B. Armentrout, J. Chem. Phys. 96 (1992) 1046.
[28] E.R. Fisher, B.L. Kickel, P.B. Armentrout, J. Phys. Chem. 97 (1993) 10204.
[29] M.T. Rodgers, P.B. Armentrout, J. Chem. Phys. 109 (1998) 1787.
[30] R.G. Gilbert, S.C. Smith, Theory of Unimolecular and Recombination Reactions, Blackwell Scientific, Oxford, 1990.
[31] D.G. Truhlar, B.C. Garrett, S.J. Klippenstein, J. Phys. Chem. 100 (1996) 12771.
[32] K.A. Holbrook, M.J. Pilling, S.H. Robertson, Unimolecular Reactions, 2nd ed., Wiley, New York, 1996.
[33] J.A. Pople, H.B. Schlegel, K. Raghavachari, D.J. DeFrees, J.F. Binkley, M.J. Frisch, R.F. Whitesides, R.F. Hout, W.J. Hehre, Int. J. Quant. Chem. Symp. 15 (1981) 269.
[34] D.J. DeFrees, A.D. McLean, J. Chem. Phys. 82 (1985) 333.
[35] T.S. Beyer, D.F. Swinehart, Commun. Assoc. Comput. Mach. 16 (1973) 379.
[36] S.E. Stein, B.S. Rabinovich, J. Chem. Phys. 58 (1973) 2438.
[37] S.E. Stein, B.S. Rabinovich, Chem. Phys. Lett. 49 (1977) 1883.
[38] M.T. Rodgers, P.B. Armentrout, J. Phys. Chem. A 101 (1997) 2614.
[39] M.T. Rodgers, K.M. Ervin, P.B. Armentrout, J. Chem. Phys. 106 (1997) 4499.
[40] E.V. Waage, B.S. Rabinovitch, Chem. Rev. 70 (1970) 377.
[41] W.J. Chesnavich, M.T. Bowers, J. Phys. Chem. 83 (1979) 900.
[42] P.B. Armentrout, in: N.G. Adams, L.M. Babcock (Eds.), Advances in Gas Phase Ion Chemistry, vol. 1, JAI Press Inc., Greenwich, CT, 1992, pp. 83–119.
[43] M.B. More, E.D. Glendening, D. Ray, D. Feller, P.B. Armentrout, J. Phys. Chem. 100 (1996) 1605.
[44] D. Ray, D. Feller, M.B. More, E.D. Glendening, P.B. Armentrout, J. Phys. Chem. 100 (1996) 16116.
[45] M.B. More, D. Ray, P.B. Armentrout, J. Phys. Chem. A 101 (1997) 831.
[46] M.T. Rodgers, P.B. Armentrout, J. Phys. Chem. A 101 (1997) 1238.
[47] M.B. More, D. Ray, P.B. Armentrout, J. Phys. Chem. A 101 (1997) 4254.
[48] M.B. More, D. Ray, P.B. Armentrout, J. Phys. Chem. A 101 (1997) 7007.
[49] P.B. Armentrout, J. Simons, J. Am. Chem. Soc. 114 (1992) 8627.
[50] M.J. Frisch, G.W. Trucks, H.B. Schlegel, G.E. Scuseria, M.A. Robb, J.R. Cheeseman, V.G. Zakrzewski, J.A. Montgomery Jr., R.E. Stratmann, J.C. Burant, S. Dapprich, J.M. Millam, A.D. Daniels, K.N. Kundin, M.C. Strain, O. Farkas, J. Tomasi, V. Barone, M. Cossi, R. Cammi, B. Mennucci, C. Pomelli, C. Adamo, S. Clifford, J. Ochterski, G.A. Petersson, P.Y. Ayala, Q. Cui, K. Morokuma, D.K. Malick, A.D. Rabuck, K. Raghavachari, J.B. Foresman, J. Cioslowski, J.V. Ortiz, B.B. Stefanov, G. Liu, A. Liashenko, P. Piskorz, I. Komaromi, R. Gomperts, R.L. Martin, D.J. Fox, T. Keith, M.A. Al-Laham, C.Y. Peng, A. Nanayakkara, C. Gonzalez, M. Challacombe, P.M.W. Gill, B. Johnson, W. Chen, M.W. Wong, J.L. Andres, C. Gonzalez, M. Head-Gordon, E.S. Replogle, J.A. Pople, Gaussian 98, Revision A.7, Gaussian, Inc., Pittsburgh, PA, 1998.
[51] J.B. Foresman, A.E. Frisch, Exploring Chemistry with Electronic Structure Methods, 2nd ed., Gaussian, Inc., Pittsburgh, PA, 1996.
[52] S.F. Boys, R. Bernardi, Mol. Phys. 19 (1970) 553.
[53] F.B. van Duijneveldt, J.G.C.M. van Duijneveldt-van de Rijdt, J.H. van Lenthe, Chem. Rev. 94 (1994) 1873.
[54] V.F. DeTuri, K.M. Ervin, J. Phys. Chem. A 103 (1999) 6911.
[55] J. Chao, K.R. Hall, K.N. Marsh, R.C. Wilhoit, J. Phys. Chem. Ref. Data 15 (1986) 1369.
[56] C. Iceman, P.B. Armentrout, Int. J. Mass Spectrom. 222 (2003) 329.
[57] A.L. McClellan, Experimental Table of Dipole Moments, W.H. Freeman, San Francisco, CA, 1963.